A comparative study for stator winding inter-turn short-circuit fault detection based on harmonic analysis of induction machine signatures

Assam Zorig, Shahin Hedayati Kia, Aissa Chouder, Abdelhamid Rabhi

Version of Record: https://www.sciencedirect.com/science/article/pii/S0378475422000325
Manuscript_bd18e11a61ba91fed4a042ccf5428f68

A Comparative Study for Stator Winding Inter-Turn Short-Circuit Fault Detection Based on Harmonic Analysis of Induction Machine Signatures

Assam ZORIG[a,b], Shahin HEDAYATI KIA[b], Aissa CHOUDER[a], Abdelhamid RABHI[b]

[a] *Laboratory of Electrical Engineering, University of Med Boudiaf ,m'sila, Algeria*
[b] *Laboratory of Modeling, Information and Systems, University of Picardie Jules Verne, Amiens, France*

Abstract

This article deals with inter-turn short-circuit fault detection in stator windings of squirrel cage induction machines. The main aim is to perform harmonic analysis of different electrical signatures namely the stator phase current, external magnetic flux and electromagnetic torque at different levels of mechanical load in order to develop an efficient fault detection approach of this kind of defect in induction machines. The proposed approach is based on the analysis of saturation related harmonics at rank $3k_1 f_s$, where k_1 is an odd number, and magnetomotive force (MMF)-related harmonics at rank $(6k_2 \pm 1)f_s$, with $k_2 = 1, 2, \cdots$ in stator phase current and stray flux and harmonics at rank $2k_2 f_s$ in electromagnetic torque. The amplitudes of these last harmonics in healthy condition are compared with 3% power supply unbalance, 16.6% (40 turns) and 33% (80 turns) levels of inter-turn short-circuit fault in frequency range from 0Hz to 2500Hz under different levels of mechanical load. Besides, the stand-still test is also investigated in this work. Simulation study is carried out based on 2.2kW squirrel cage IM using finite element method (FEM). This method provides accurate and inexpensive tool for evaluating the performance of induction machine under healthy and faulty conditions. The obtained results demonstrate that the stray flux is the most

Email addresses: assam.zorig@univ-msila.dz (Assam ZORIG), Shahin.Hedayati.Kia@u-picardie.fr (Shahin HEDAYATI KIA), aissa.chouder@univ-msila.dz (Aissa CHOUDER), abdelhamid.rabhi@u-picardie.fr (Abdelhamid RABHI)

sensitive signature to the stator winding inter-turn short-circuit fault, and it is robust against the power supply unbalance in comparison with both stator current and electromagnetic torque.

Keywords: Induction motors, Modeling, Finite element method (FEM), Diagnostic, harmonics, Monitoring, Signal processing.

---

1. Introduction

Online condition monitoring (CM) of induction machines (IMs), which are prime movers used in the industries, is essential for their safe and reliable operation. The main aim of CM is to achieve optimal use of these components, avoid unexpected downtime and consequently avoiding economic losses. From this point of view, fault detection and diagnosis of incipient mechanical and electrical faults have been widely investigated to develop advanced condition-based maintenance (CBM) systems [27], [11]. Based on the survey results provided by IEEE and EPRI on medium size IMs, 28% and 36% of faults in this class of electrical machines are stator related [18]. Main types of stator winding faults are turn-to-turn, coil-to-coil, phase-to-phase, short-circuit between turns of all three phases, coil-to-ground and open-circuit when winding gets break [13]. Particularly, the stator winding inter-turn short-circuit may occur due to the degradation of isolation in case of moisture, system surge, overload or overheating owing to fan blocking or other kinds of faults like broken rotor bars and cracked end rings in cage IMs [39]. The developed fault detection techniques are commonly based on the analysis of signatures such as stator phase current and voltage, the estimation or computation of the equivalent impedance, the active and reactive power, the vibration, the electromagnetic torque estimation and the external magnetic field [29]. Particular attention is dedicated to the noninvasive techniques so-called machine electrical signature analysis (MESA), which need the least modifications on the system under monitoring [40], [6], [10]. The frequency-domain analysis is an efficient approach of fault detection since each kind of fault induces its characteristic frequency in the measured signal, which can be well explored in most of the cases in the frequency domain [7]. MESA is a well-known technique for stator winding inter-turn short-circuit fault diagnosis, as it was shown [4], [1]. For instance, air-gap flux harmonics

are initially localized in the stator current spectrum for fault detection [34]:

$$f_{sc-1} = \left(\frac{n}{p}(1-s) \pm k_1\right) f_s = n f_r \pm k_1 f_s \tag{1}$$

with f_s: supply frequency, f_r: rotor rotation frequency, $n = 1, 2, 3, \cdots$, and $k_1 = 1, 3, 5, \cdots$, p=pole-pairs, s=slip. The principal slot harmonics given by (2) can be analyzed as well for detection of stator winding inter-turn fault as it was indicated [28]:

$$f_{PSH-1} = \left(\frac{k_2 R}{p}(1-s) \pm v\right) f_s \tag{2}$$

where k_2 is any positive integer ($k_2 = 1, 2, 3, \cdots$) and R is the number of rotor slots, v is the time harmonic order ($v = \pm 1, \pm 3, \pm 5, \cdots$). This last relation can be generalized considering all time harmonics as [31]:

$$f_{PSH-2} = \left(\frac{j_{rt} R}{p}(1-s) \pm 2 j_{sa} \pm i_{rt}\right) f_s \tag{3}$$

with j_{rt}, j_{sa} and i_{rt} are integers. The amplitude of main fault frequency components in (3) are studied. Although a substantial increase in harmonics amplitudes due to the fault, it is difficult to determine the fault severity since this last parameter is totally affected by magnetic saturation, stator winding inherent unbalance as well as power supply voltages unbalance [7]. The localization of air-gap flux and rotor slot harmonics in the stator current spectrum needs the prior knowledge of the rotor mechanical speed as it can be clearly observed in (1), (2) and (3). In this respect, several works introduce third harmonic $3f_s$ [3], [12] and $\pm 3f_s$ [38] in the stator current spectrum of faulty IMs. It was also illustrated that $2f_s$ can be detected in the modulus of extended park vector (EPV) [3] which is the shifted version of $3f_s$ harmonic. The usage of external magnetic field measurement is another technique with the simplicity of implementation which senses indirectly the stator and rotor currents harmonics and gives the ability of both stator and rotor faults detection [24], [14], [23]. The proposed harmonics related to the stator fault in axial leakage flux signature is initially proposed [24]:

$$f_{sc-3} = \left(k_3 \pm \frac{n}{p}(1-s)\right) f_s \tag{4}$$

with $k_3 = 1, 3$ and $n = 1, 2, 3, \cdots, 2p - 1$. In this regard, it is found that the stator fault give rises of low order harmonics with $k_3 = 1$ and $n = 1, 2$ in the spectrum of axial leakage flux and finally the third harmonic is proposed for fault detection [40]. Moreover, it was illustrated that time harmonics namely $15f_s$ and $17f_s$ are good indicators of this kind of fault [25], [33], [10]. Besides, many researchers used the instantaneous torque as a fault indicator in induction motors [36, 9, 22, 26, 20, 30, 8, 21]. It is important to mention that there are differences in the instantaneous torque response under stator and rotor faults [36]. It is well known in electrical machines theory that the first additional current component introduced by an electric or magnetic stator asymmetry produces a negative sequence component at $-f_s$ frequency. The interaction of this frequency component with the main rotor current frequency produces a torque pulsation and electromagnetic forces at $2f_s$ [22, 26, 21, 32, 17, 16]. In this paper, a comparative study has been performed based on the harmonic analysis of electrical signatures namely the stator phase current, the external magnetic flux and the electromagnetic torque in [0Hz - 2500Hz] frequency bandwidth for inter-turn short-circuit fault detection in stator winding of IMs. It is carried by amplitude analysis of saturation harmonics $3k_1f_s$, where k_1 is an odd number, and MMF-related harmonics $(6k_2 \pm 1)f_s$, with $k_2 = 1, 2, \cdots$ to investigate the most sensitive electrical signatures to the fault and examine its robustness to the power supply unbalance perturbation. To assess the validity of the proposed method, the numerical simulation using finite element method (FEM) is carried out for a 2.2kW squirrel cage induction machine in working condition of healthy, unbalanced power supply and two levels of 16.6% (40 turns) and 33% (80 turns) inter-turn short-circuit respectively at different level of loads and stand-still case. Moreover, the electromagnetic torque harmonic analysis using $2k_2f_s$ frequency components in [0Hz - 1000 Hz] frequency bandwidth is performed at different levels of the load.

2. Modeling of Stator Winding Intern-Turn Fault

The development of an accurate model in both healthy and faulty conditions is a crucial stage of any fault diagnosis procedure. The most precise approach of 2D/3D modeling for this aim is relied on multiphysics FEM which is a well-known mathematical tool for solving the combined magnetic and electric numerical problems [15], [2], [19]. In this respect, the spatial distribution of the stator winding, non uniformity of the air-gap due to sta-

tor and rotor slots, non-linearity characteristics of the stator and rotor core materials, skin effects and eddy currents can be considered for 2D modeling of IMs in both healthy and faulty conditions. Similarity of numerical simulation results to the experiments allows setting up a reliable signal-based fault diagnosis procedure [35]. It provides variables such as the electromagnetic field distribution, the flux linkage, the flux density, the stator and rotor phase currents, the rotor rotation speed and the electromagnetic torque knowing precise geometry and physical characteristic of both stator and rotor structures and materials respectively. The equation to be resolved by the FEM is defined as follows:

$$\sigma_e \frac{\partial \vec{A}}{\partial t} + \overrightarrow{rot}\left(\frac{1}{\mu rot(\vec{A})}\right) = J + \overrightarrow{rot}(\vec{H}) \tag{5}$$

where H is the magnetic field $[A/m]$, A is the magnetic vector potential $[Weber/m]$, is the electric current density $[A/m]$, σ_e the electrical conductivity $[S/m]$, μ is the magnetic permeability $[H/m]$. Fig. 1.a shows the geometry of the IM with its related electrical circuit. A search coil (stray flux sensor) with 1200 turns is placed at a distance of $110mm$ from the center of IM for measuring the induced voltage of radial external magnetic field. An

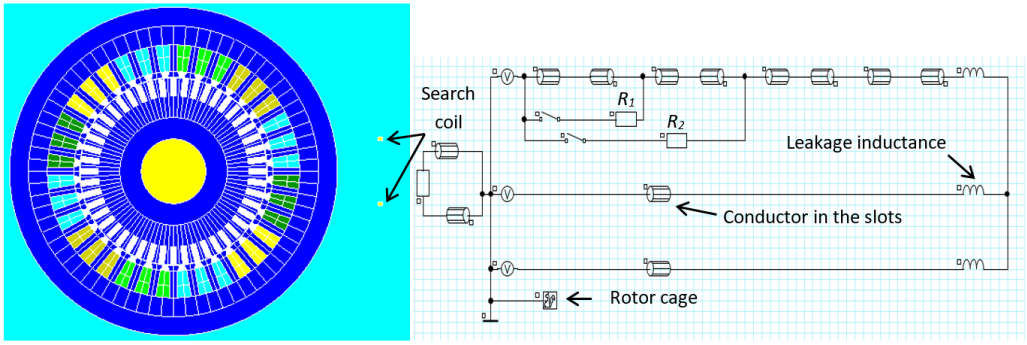

(a) (b)

Figure 1: FEM analysis for magnetic field computation (a) geometry of IM (b) electrical circuit model.

electrical circuit which consists of a three-phase supply source, a three-phase stator winding and three leakage inductances are coupled to the finite element model (Fig. 1.b). Two resistors $R_1 = R_2 = 3\Omega$ are placed to create two levels of inter-turn short-circuit fault of 16.6% and 33% respectively in

one phase of the stator winding. In this work, the value of the resistor R_1 is chosen to allow the limit of the short circuit current and to simulate a incipient winding faults. Accordingly, the safety systems do not react to this fault because we have a slight increase in phase currents and the induction motor can still run .

Table 1 provides main electrical characteristics and geometries of both stator and rotor structures for FEM analysis of the IM under study.

		Value	Unit
Machine	Power	2.2	kW
	Voltage	400	V
	Current	4.24	A
	Speed	1440	rpm
Stator	Number of phases	3	
	Connection type	Y	
	Number of slots	36	
	Internal diameter	99	mm
	External diameter	173	mm
Rotor	Airgap length	0.33	mm
	Number of bars	48	
	Internal diameter	34	mm
	External diameter	98.1	mm

Table 1: Electrical characteristics and geometries of both stator and rotor structures for FEM analysis

The search coil sensor, located in vicinity of IM, allows measuring the external magnetic flux which pass through it [37]. Furthermore, it delivers an output voltage which is equal to the derivative of the magnetic flux. This means that only the measurement of time-variable fields are possible. For many industrial applications, it is crucial to detect the electrical and mechanical faults in electrical machines without stopping the operation, and hence it is interesting to use the non-invasive methods [25]. Moreover, the measurement of stator phase current is not always possible, since often the winding may not be always available. In this regard, several works investigate the possibility to employ a search coil to monitor the conditions of medium and small size IMs [5].

3. Numerical Simulation Results

In Figs 2.a and 2.b, shown below, the distribution of magnetic flux lines inside the IM in both healthy and unbalanced voltage supply conditions are represented. It is worth to mention here that this distribution is almost symmetrical in both cases. Nevertheless, in Figs 2.c and 2.d we notice the existence of distortions in the distribution of magnetic flux lines in faulty conditions. Similarly, in Figs 3.a and 3.b it is illustrated that the outside magnetic field distribution for healthy and unbalanced voltage supply cases are symmetrical whereas they are highly distorted in the case of 16.6% and 33% inter-turn stator winding short-circuit fault; (see Figs. 3.c and 3.d).

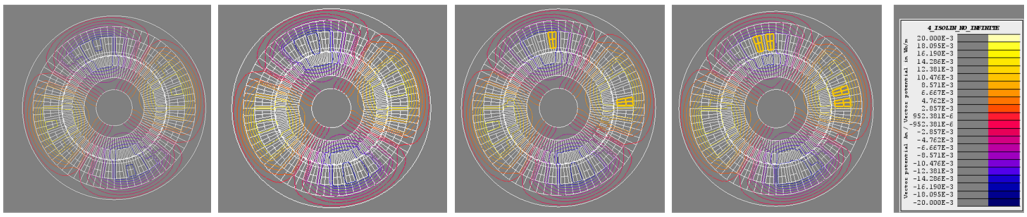

(a) (b) (c) (d)

Figure 2: Lines of inside magnetic flux: (a) healthy condition (b) 3% voltage unbalance supply (c) 16.6% inter-turn stator winding short-circuit (d) 33% inter-turn stator winding short-circuit.

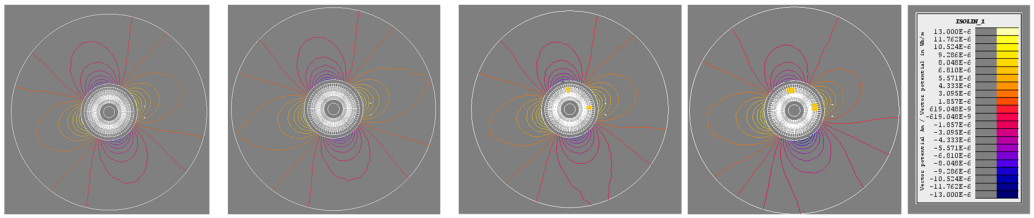

(a) (b) (c) (d)

Figure 3: Lines of outside magnetic field: (a) healthy condition (b) 3% voltage unbalance supply (c) 16.6% inter-turn stator winding short-circuit (d) 33% inter-turn stator winding short-circuit.

In Figs 4 to 7 it is shown the time evolution of three-phase stator current, stray flux and electromagnetic torque at healthy condition, unbalanced voltage supply, 16.6% and 33% inter-turn stator winding short-circuit faults respectively.

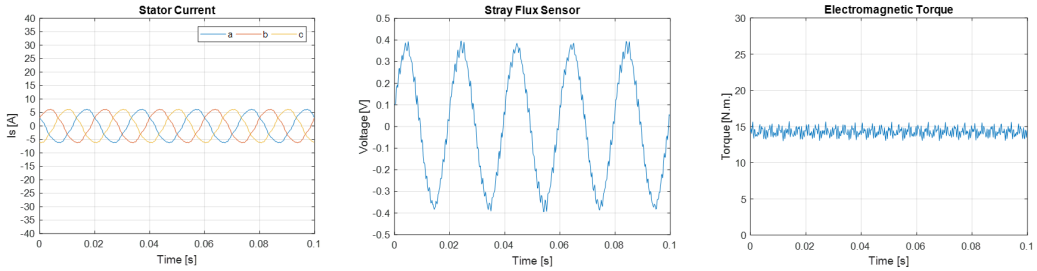

Figure 4: Stator current, stray flux sensor and electromagnetic torque signals at full load in healthy condition.

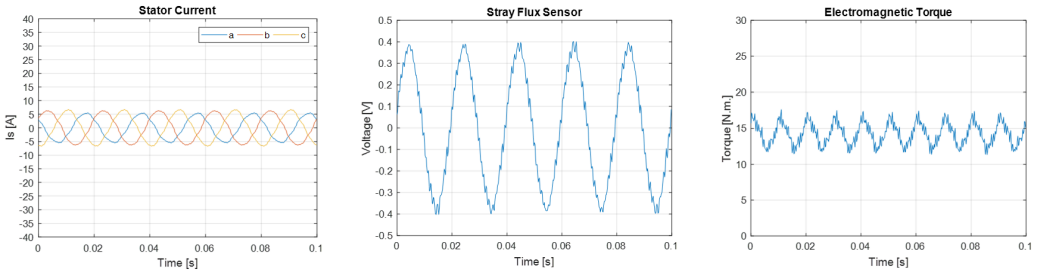

Figure 5: Stator current, stray flux sensor and electromagnetic torque signals at full load at 3% voltage unbalance supply condition.

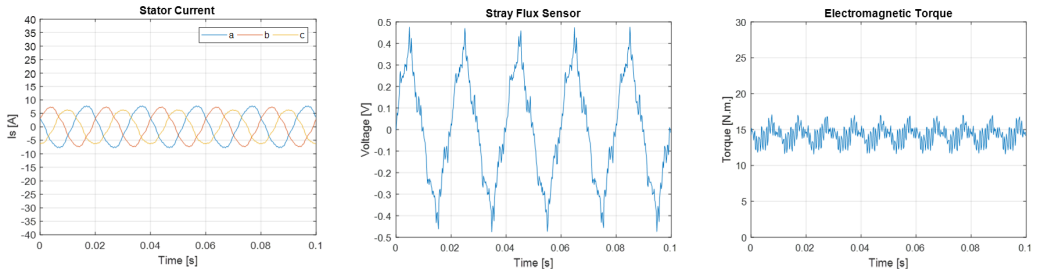

Figure 6: Stator current, stray flux sensor and electromagnetic torque signals at full load at 16.6% inter-turn stator winding short-circuit condition.

In the case of unbalanced voltage supply (see Fig. 5), it can be noticed the apparition of fluctuations in the stator current in comparison with healthy case. Also in the faulty phase current, shown in Fig. 6 and 7,it is clearly visible an increase of the peak amplitude. The currents in the other phases also increase, but the increase is less significant compared to the faulty phase. To confirm this kind of fault condition, the induced voltage of stray flux sensor include sufficient information about the motor condition. If the machine

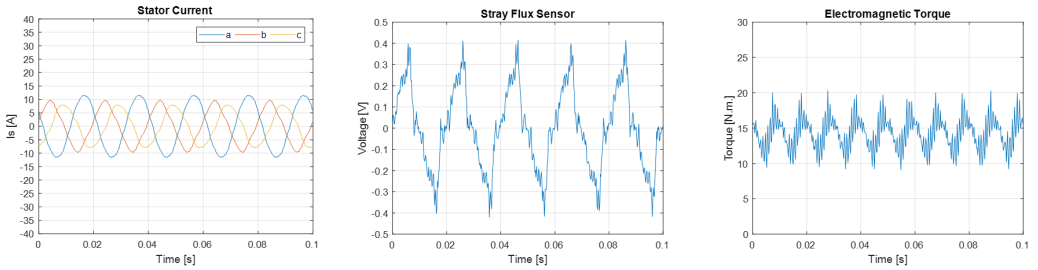

Figure 7: Stator current, stray flux sensor and electromagnetic torque signals at full load at 33% inter-turn stator winding short-circuit condition.

is affected by a short circuit fault (see Fig.6 and 7), it can be observed a very significant modification in the temporal variation of induced voltage compared with healthy machine (see Fig. 4) and in unbalanced voltage supply case (see Fig. 5). In addition the fluctuations are more accentuated when the number of short circuit turns increase. The torque variation at healthy condition is given in Fig. 4 where we notice the existence of small oscillations; generally generated by the motor slots. The existence of an unbalanced voltage and stator fault generates the unbalance of the interaction rotor–stator electromagnetic force which induce torque ripples that can be observed at frequency $2f_s$ (see Figs. 5 to 7).
Frequency analysis of stator current, stray flux and electromagnetic torque at full load condition are given in Figs. 8 to 11. This analysis are collected for the case of healthy, unbalanced voltage supply, 16.6% and 33% inter-turn short-circuit respectively.

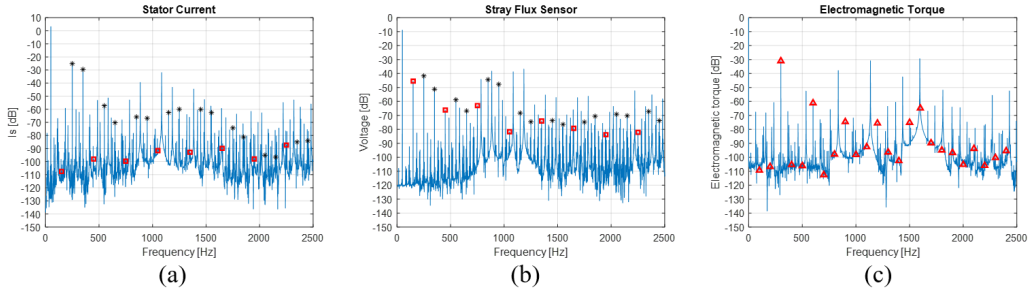

Figure 8: Healthy condition spectra: (a) Stator current (b) Stray flux sensor (c) Electromagnetic torque. '$*$': $3kf_s$ – '$\square$': $(6k \pm 1)f_s$ – 'Δ': $2kf_s$

From the obtained results, some remarks have to be emphasized. Firstly,

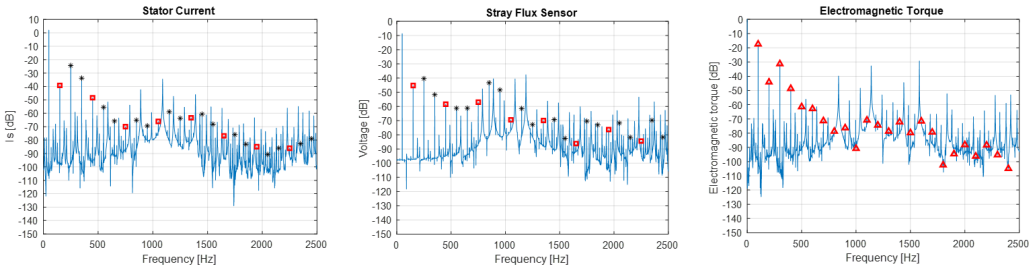

Figure 9: Voltage unbalance condition spectra: (a) Stator current (b) Stray flux sensor (c) Electromagnetic torque. '$*$': $3kf_s$ – '$\square$': $(6k \pm 1)f_s$ – 'Δ': $2kf_s$

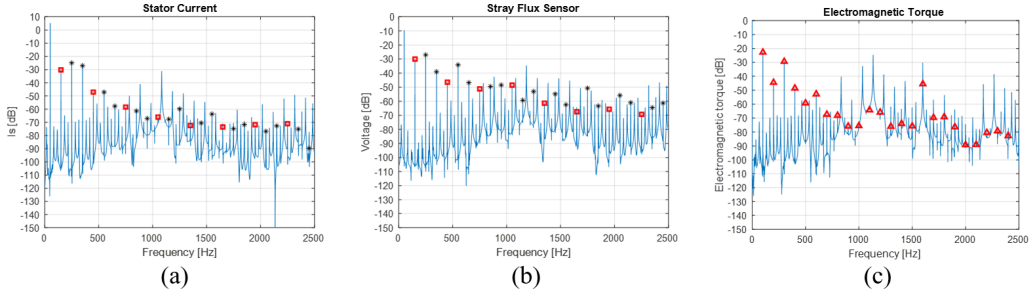

Figure 10: 16.6% inter-turns short-circuit fault spectra: (a) Stator current (b) Stray flux sensor (c) Electromagnetic torque. '$*$': $3kf_s$ – '$\square$': $(6k \pm 1)f_s$ – 'Δ': $2kf_s$

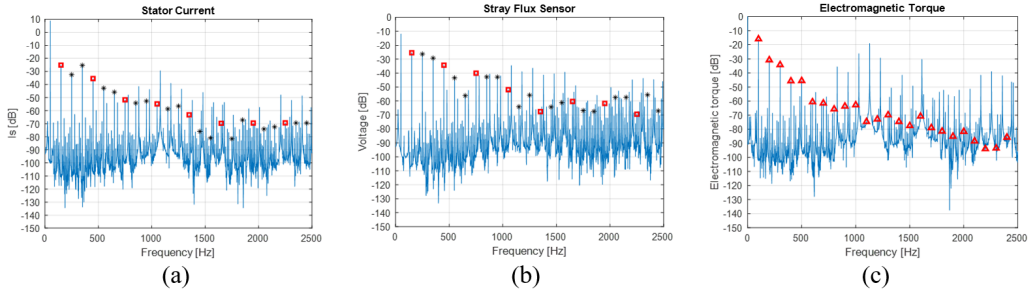

Figure 11: 33% inter-turns short-circuit fault spectra: (a) Stator current (b) Stray flux sensor (c) Electromagnetic torque. '$*$': $3kf_s$ – '$\square$': $(6k \pm 1)f_s$ – 'Δ': $2kf_s$

the stator MMF-related harmonics at ranks $(6k_2 \pm 1)$ (such as $250\text{Hz}, 350\text{Hz}, , \cdots$) and the saturation related harmonic $3k_1 f_s$ (such as $150\text{Hz}, 450\text{Hz} \cdots$) are present in current and stray flux spectrum. Also harmonics at ranks $2k_2 f_s$ (such as $100\text{Hz}, 200\text{Hz}, \cdots$) in electromagnetic torque spectrum can be ob-

served. All these fault signatures will be analyzed in the next sections.

4. Stator Current Analysis

Based on FEM simulations, the ability of current signature analysis method (MCSA) to detect the inter-turn short circuit in the stator winding faults is assessed. These assessments were carried out in order to investigate the effect of load changes on the components that indicate the shorted turns. The considered load levels are: no-load and 25% ,50%, 75% of the rated load respectively and at full load condition. In Fig. 12, the saturation related harmonics at ranks $(3k_1 f_s)$ and the stator MMF-related harmonics at ranks $(6k_2 \pm 1)f_s$ of stator current are presented for the both cases of healthy and faulty IM. The consequence of the inter-turn short circuit fault is the increase in saturation related harmonics amplitude. In particular, the amplitude of harmonics at frequencies: 150Hz, 450Hz, 750Hz, and 1050Hz increases under different load values. The amplitude of the other harmonics (i.e: at 1350Hz, 1650Hz, 1950Hz, and 2250Hz) increases when the motor is loaded but decreases at no load condition. In order to better quantifying the net increase of harmonics amplitude, the sensitivity of saturation related harmonics of stator current, under different load values, have been presented in Fig. 13. It is worth to mention here that the sensitivity is computed as the difference of each harmonic between faulty and healthy condition. It can be observed that the harmonics at 150Hz, 450Hz and 750Hz (3^{rd},9^{th} and 11^{th}), are more sensitive to the inter-turn short-circuit fault. In addition, the choice of the threshold of sensitivity in the case of 16.6% inter-turn short-circuit fault must be larger than the effect of load changes on the magnitude of these harmonics at healthy condition. In the same figure (case (a)), it can also be observed that these harmonics increase in the case of unbalanced voltage supply at different load values. For instance, the (3^{rd}) harmonic increase at full load by a net value of +68.4dB. These results clearly demonstrate that is difficult to use these signatures for discrimination between the effects of stator inter-turn fault and those due to unbalanced supply voltages. In the stator MMF-related harmonics, only the harmonics 350Hz, 550Hz and 650Hz increase under different load conditions in the case of the inter-turn short-circuit fault .The other harmonics have slight differences where half of them increase while the other half decrease. The sensitivity of these harmonics signatures under different load conditions are presented in Fig. 14. It can be observed that only the 11^{th} harmonic (550Hz) exceeds the level of +10

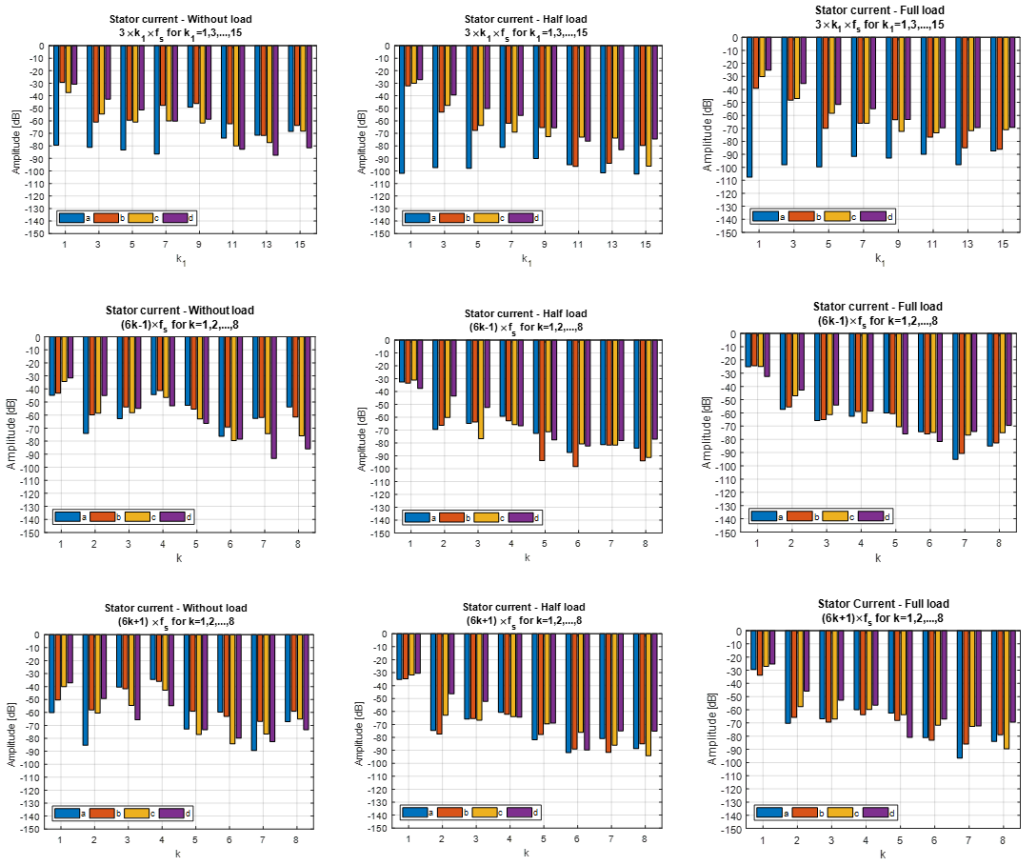

Figure 12: Stator current harmonics, (a) healthy machine (b) 3% unbalanced voltage, (c) 16.6% inter-turn stator winding short-circuit (d) 33% inter-turn stator winding short-circuit.

dB in the case of 16.6% inter-turn short-circuit fault. Moreover, in terms of detection, the results have proved that MMF-related harmonics have low sensitivity compared to saturation related harmonics.Consequently, it cannot be used as a specific signature of the occurrence of inter-turn short circuits fault.

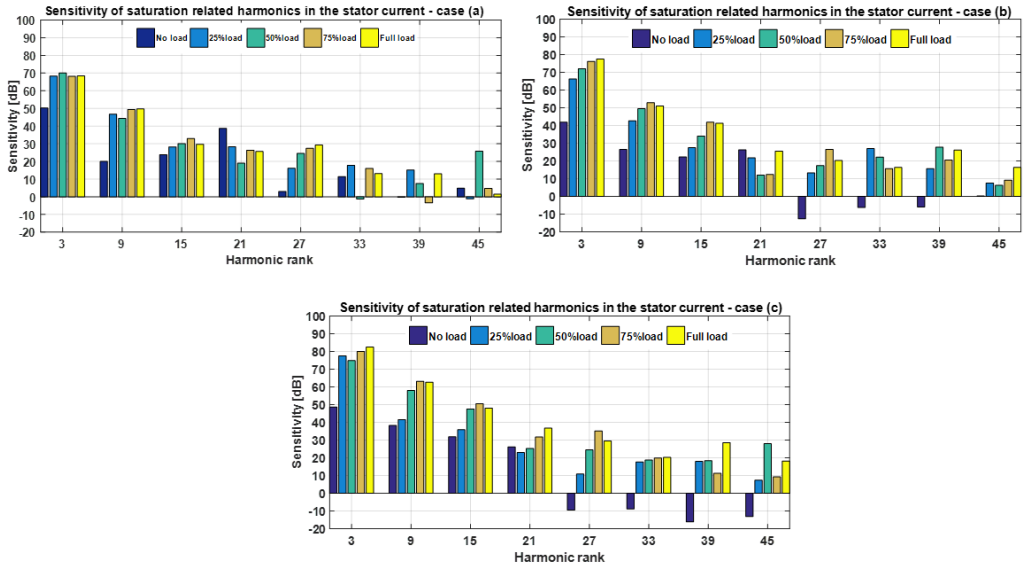

Figure 13: Sensitivity of saturation related harmonics in the stator current, (a) 3% unbalanced voltage supply, (b) 16.6% inter-turn stator winding short-circuit, (c) 33%inter-turn stator winding short-circuit.

5. Stray Flux Analysis

In the following section, harmonics analysis of the stray flux will be highlighted. In Fig.15, it is reported the saturation related harmonics at rank $3k_1 f_s$ and the MMF-related harmonics at ranks $(6k_2 \pm 1)f_s$ of the stray flux under different loads condition, for both healthy and faulty IM. The results show a clear increase in the amplitude of saturation related harmonics with inter-turn short circuit fault at loaded IM cases. When the IM is not loaded, the harmonics at frequencies 150Hz, 450Hz, 750Hz, and 1050Hz show the same sensitivity. However, the harmonics at frequencies 1350Hz, 1650Hz show a low sensitivity and the harmonics of 1950Hz and 2250Hz decrease in magnitude with inter turn short circuits faults.

In Fig. 16, it is presented the sensitivity of saturation related harmonics in stray flux under different load conditions. The harmonics showing the highest level of significance are 150Hz, 450Hz, 750Hz, and 1050Hz. In this case, we can clearly see that the 3^{rd} harmonic (150Hz) increases between +13.4dB to +18.6dB in the case of 16.6% short-circuit faults.In counterpart the sensitivity of this component have changed between -0.1dB to +1.7dB in the case of unbalanced voltage supply. This change in the magnitude of this

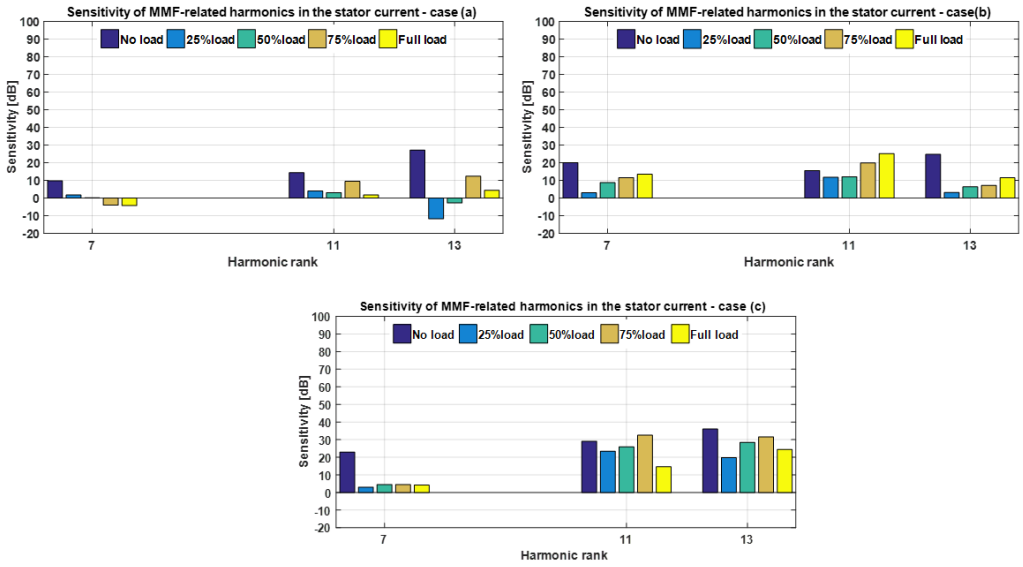

Figure 14: Sensitivity of MMF-related harmonics in the stator current, (a) 3% unbalanced voltage supply, (b) 16.6% inter-turn stator winding short-circuit, (c) 33% inter-turn stator winding short-circuit.

component is negligible in comparison to the case of inter-turn short circuits fault. Also it is found that the load variation does not has a significant effect on the sensitivity of this harmonic. The sensitivity of the 9^{th} harmonic (450Hz) in the case of 16.6% inter-turn short-circuit faults has varied between +23.5dB to +36.6dB under different loads values. However in the case of unbalanced voltage supply, it has varied only between +4.4dB to +9.6dB. For the sensitivity of 15^{th} harmonic (750Hz) has varied between +13dB to +19.5dB in the presence of 16% inert-turn short-circuit fault and has small increase of less than +4.6dB in unbalanced voltage supply case. Finally, the sensitivity of 21^{th} harmonic (1050Hz) has also increased between +13.4dB to +25.2dB in the presence of 16% inert-turn short-circuit fault and less than +7.9dB in unbalanced voltage supply case. These results indicate that these specific saturation related harmonics of stray flux such as (150Hz, 450Hz, 750Hz and 1050Hz) are good indicators of inter-turn short circuit fault and exhibit low sensitivity to unbalanced voltage supply and load variation effect. Moreover these harmonics signatures have a high ability to distinguish between two faults that lead to the reliability of the diagnosis system.

for MMF-related harmonics of the stray flux the effect that allows the

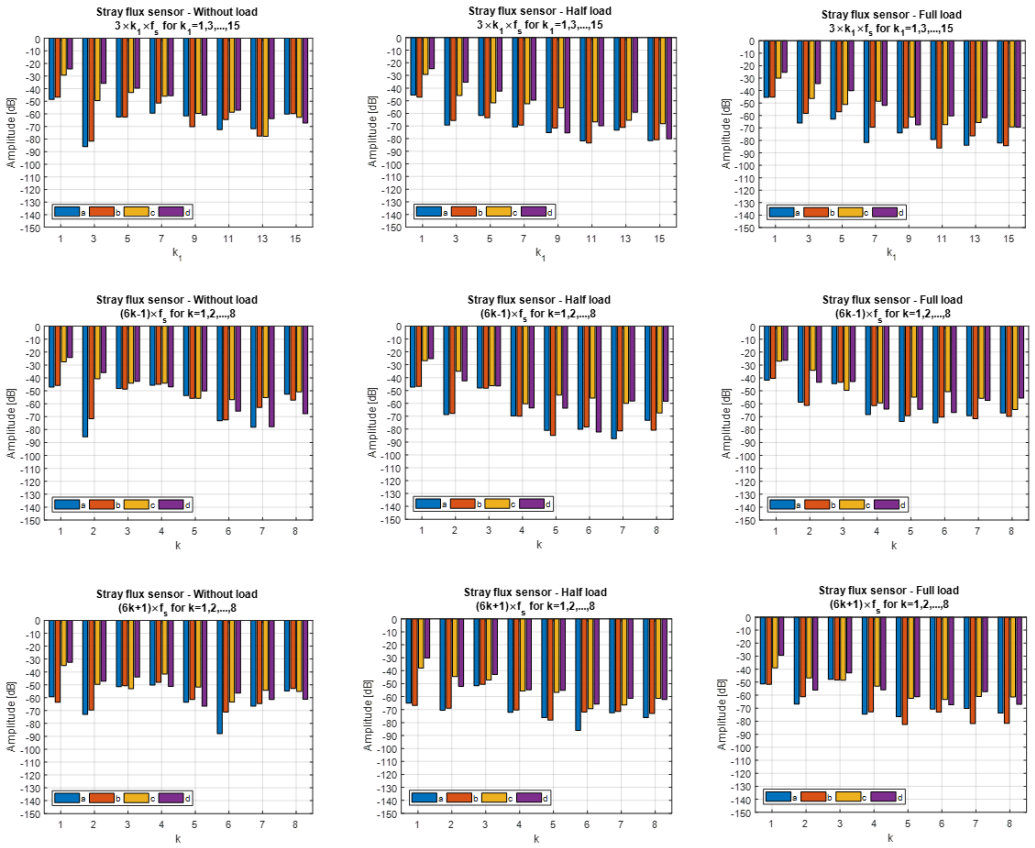

Figure 15: Stray flux sensor harmonics, (a) healthy machine (b) 3% unbalanced voltage, (c) 16.6% inter-turn stator winding short-circuit, (d) 33%inter-turn stator winding short-circuit.

detection of the inter-turn short circuit fault under different load conditions can be localized in the harmonics (250Hz,550Hz, and 2050Hz) in $(6k_2 - 1)f_s$ and the harmonics (350Hz, 650Hz, 1850Hz and 2150Hz) in $(6k_2+1)f_s$, which are increasing at different loads values. Moreover, it can be observed that these harmonics exhibit a low sensitivity to the unbalanced voltage supply. The sensitivity of the selected MMF-related harmonics of the stray flux,under different loads values, are presented in Fig. 17. It can be observed that the harmonics which present the highest level of significance are 5^{th}, 7^{th}, 11^{th} and 13^{th} harmonics (250Hz, 350Hz, 550Hz and 650Hz). The sensitivity of the 5^{th} and 7^{th} harmonic have varied between +10dB to +24.6dB in the case of 16.6% inter-turn short-circuit faults and only by less than +1.5dB in the

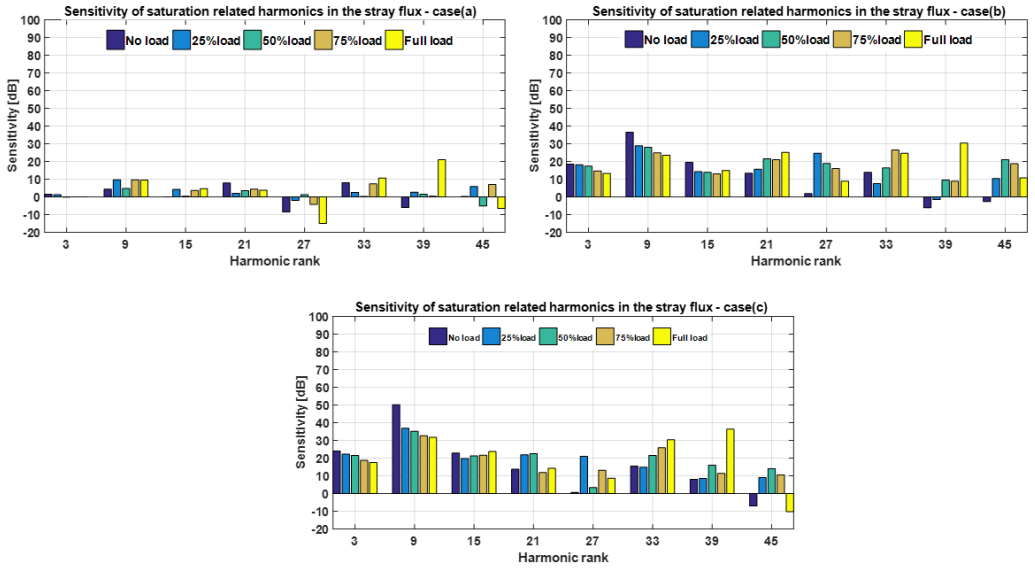

Figure 16: Sensitivity of saturation related harmonics in the stray flux, (a) healthy machine (b) 3% unbalanced voltage, (c) 16.6% inter-turn stator winding short-circuit, (d) 33%inter-turn stator winding short-circuit.

case of unbalanced voltage supply. The 11^{th} and 13^{th} harmonics present a high sensitivity between +22.2dB to +45.6dB in the case of 16.6% inter-turn short-circuit faults. It can also be seen that the sensitivity of these harmonics, in the case of unbalanced voltage supply, take a negative or small sensitivity values (less than 3dB), except at no load condition where the 11^{th} harmonic increases with 14dB. In addition, it is worth to mention here that these signatures of MMF-related harmonics of stray flux reveal also good diagnostic potential, which is not the case for the MMF-related harmonics of stator current.

6. Stand still test

In this section, the IM is simulated at standstill test where the space harmonics are not present. In this case, the saturation related harmonics of stator current and stray flux, for healthy and faulty IM are presented in Fig. 18. The sensitivity of these harmonics are presented in Tables 2 and 3. It is clear that these harmonic signatures of 150Hz, 450Hz, 750Hz and 1050Hz have been significantly increased, specifically in stator current. These results

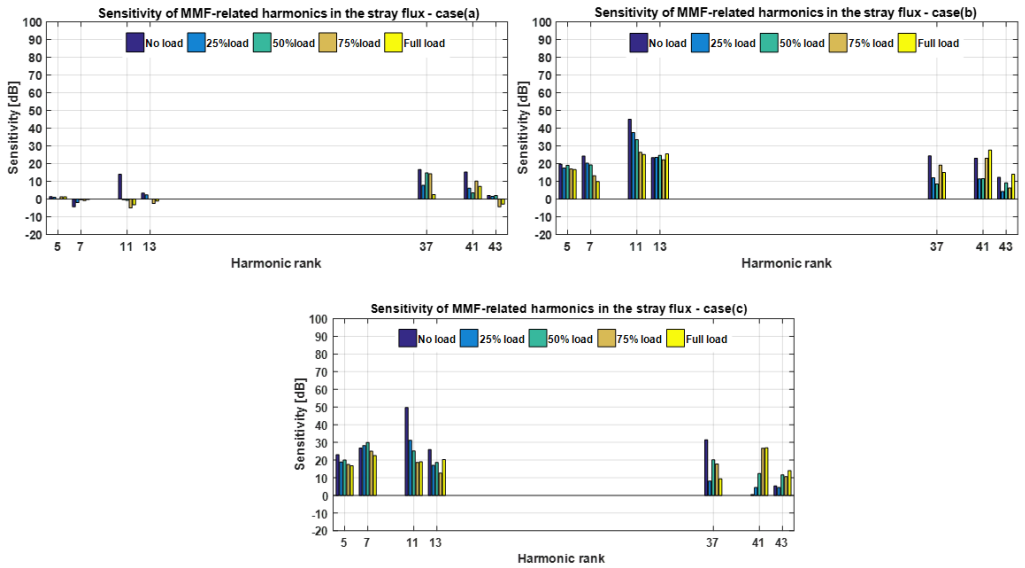

Figure 17: Sensitivity of MMF-related harmonics in the stray flux, healthy machine, (b) 3% unbalanced voltage, (c) 16.6% inter-turn stator winding short-circuit, (d) 33%inter-turn stator winding short-circuit.

Motor cases	Harmonics sensitivity (dB)							
Harmonic rank	3	9	15	21	27	33	39	45
a	+59.5	+43.3	+34.9	+24.4	+16.9	-10.9	17.2	+2.1
b	+69	+55.2	+41.7	+23.8	+24.8	+24.7	+10.3	-2.7

Table 2: Saturation harmonics sensitivity of the stator current at standstill, (a) 16.6% inter-turn stator winding short-circuit, (b) 33% inter-turn stator winding short-circuit.

are in good agreement with previous works. The MMF-related harmonics at ranks $(6k_2 \pm 1)f_s$ of stator current and stray flux are presented in Fig. 18. The sensitivity of these harmonics are presented in Tables 4 and 5. Also, we note here that the MMF-related harmonics in stator current present low sensitivity with inter-turn short-circuit faults. It can be seen a small increase in magnitude of harmonics found previously (i.e : 350Hz, and 650Hz), and decrease in magnitude of harmonic 550Hz. For the sensitive MMF-related harmonics of the stray flux found previously (250Hz, 350Hz, 550Hz, and 650Hz) and reported in Table 5 have increased with inter turn short circuits fault, except for the harmonic 350Hz.

Motor cases	Harmonics sensitivity (dB)							
Harmonic rank	3	9	15	21	27	33	39	45
a	+3.7	+12.6	+21	+21.2	+18.4	+19.2	+18.5	+17.7
b	+10.8	+10.3	+14.2	+20.7	+2.70	+8.3	+13.7	+11.7

Table 3: Saturation harmonics sensitivity of induced voltage at standstill, (a) 16.6% inter-turn stator winding short-circuit, (b) 33% inter-turn stator winding short-circuit.

Motor cases	Harmonics sensitivity (dB)		
Harmonic rank	7	11	13
a	+0.7	-2.8	+2.2
b	+0.5	+6.3	+15.3

Table 4: Sensitivity of sensitive MMF-related harmonics of stator current at standstill, (a) 16.6% inter-turn stator winding short-circuit, (b) 33% inter-turn stator winding short-circuit.

Motor cases	Harmonics sensitivity (dB)							
Harmonic rank	5	7	11	13	37	41	43	47
a	+11.2	-2.8	+20.8	+21.4	+12.1	+15.1	+13.2	+7.4
b	+11.5	-7.2	+19.5	+10.9	+1.2	+8.9	+9.8	+24.2

Table 5: Sensitivity of sensitive MMF-related harmonics of induced voltage at standstill, (a) 16.6% inter-turn stator winding short-circuit, (b) 33% inter-turn stator winding short-circuit.

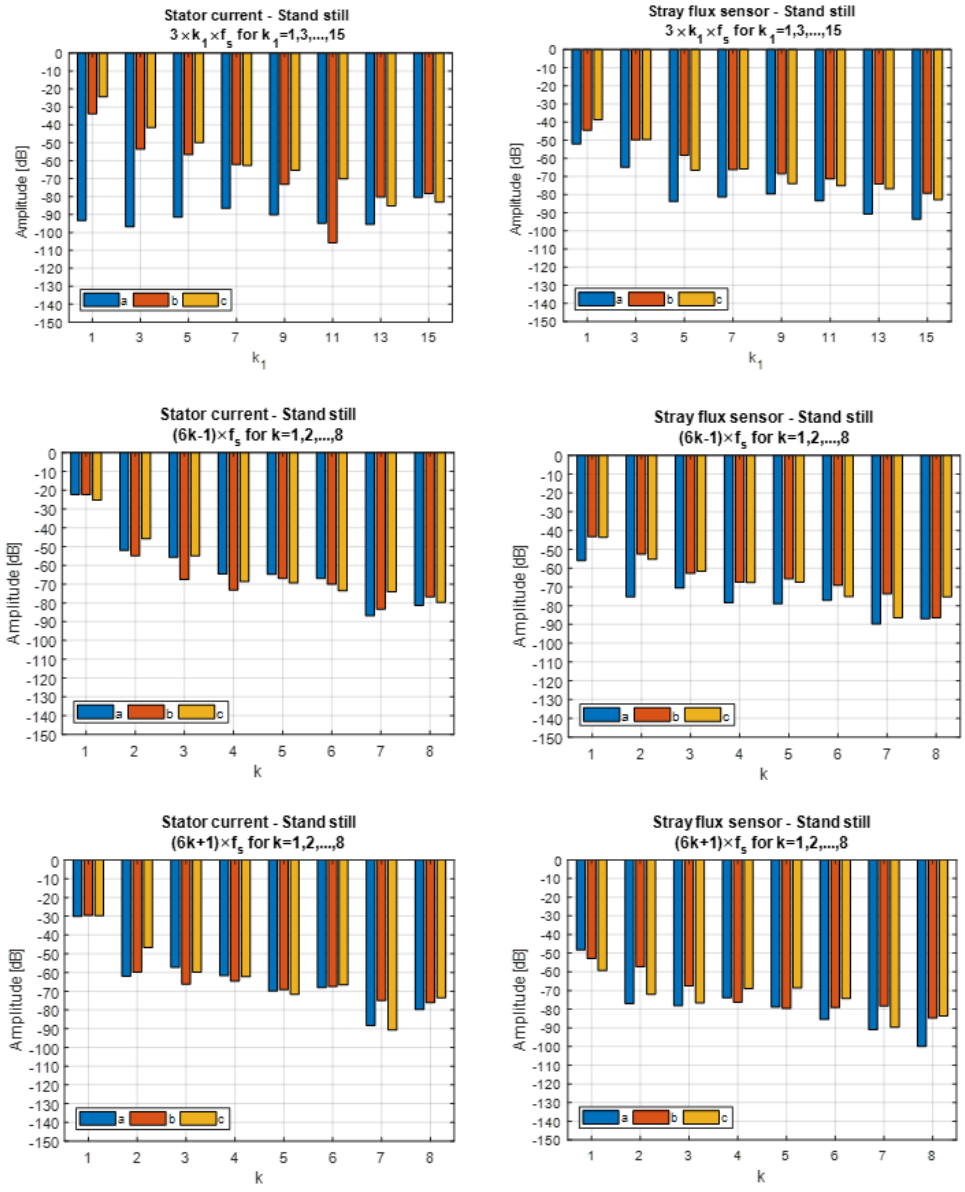

Figure 18: Stator current and stray flux sensor harmonics at stand still condition, (a) healthy machine, (b) 16.6% inter-turn stator winding short-circuit, (c) 33% inter-turn stator winding short-circuit.

7. Electromagnetic Torque Analysis

The electromagnetic torque is produced by the interaction of flux linkages and the currents of the IM. It is characterized by harmonic content that de-

pendents on several causes, such as the stator and rotor MMF, the saturation and the slot related harmonics. It has already been noted that the monitoring of the electromagnetic torque has been used for the detection of IM faults. In this work, it is proposed to detect the short circuit turn fault by observing harmonics at $2k_2f_s$ in the electromagnetic torque spectrum. These harmonics (such as, 100Hz, 200Hz, 300Hz, 400Hz, 500Hz, 600Hz, 700Hz, 800Hz, 900Hz) are presented in Fig.19 in case of healthy and faulty IM under different load values. It is clear that the most sensitive harmonics that increase with the presence of the inter-turn short-circuit fault and unbalanced voltage supply are: 100Hz, 200Hz, 400Hz, 500Hz, 700Hz, 800Hz. In the other hand, the harmonics 300Hz, 600Hz, and 900Hz show a low sensitivity. Moreover, the harmonic $2f_s = 100$Hz, is typically known as an indicator of the presence of inter-turn short circuits fault. The obtained results also have confirmed this behavior. The sensitivity of electromagnetic torque harmonics which present the highest level of significance, under different load values, are presented in Fig. 20. The obtained results show that the 2^{nd} and of 8^{th} harmonic are the most sensitive. The amplitude of 2^{nd} harmonic at the rated load has largely increased by +86.6dB and by +92dB in the case of 16.6% inter-turn short circuit fault and unbalanced voltage supply respectively. At no load condition, this component has a sensitivity of +52.7dB and +55.9dB in the case of 16.6% inter-turn short circuit fault and unbalanced voltage supply respectively. Also the 8^{th} harmonic (400Hz) presents a high sensitivity under different load values, which are excited increasing their magnitude of around 50dB in the case of 16.6% inter-turn short circuit fault and unbalanced voltage supply. The 4^{th} harmonic (200Hz) presents a sensitivity around +60dB when the machine is rotating with a loaded shaft, however, when the machine rotates without load, this component has a less sensitivity (+14.9dB). The same remark applies to the components 10^{th} and 14^{th}, which have a sensitivity at no load less than in the case of loaded IM. Finally, the 16^{th} harmonic has a relatively a low sensitivity between +13.7dB to +30dB. The results obtained show that the electromagnetic torque method has a difficult to discriminate between the unbalanced voltage supply and inter-turn short circuit fault when the second is characterized by low severity.

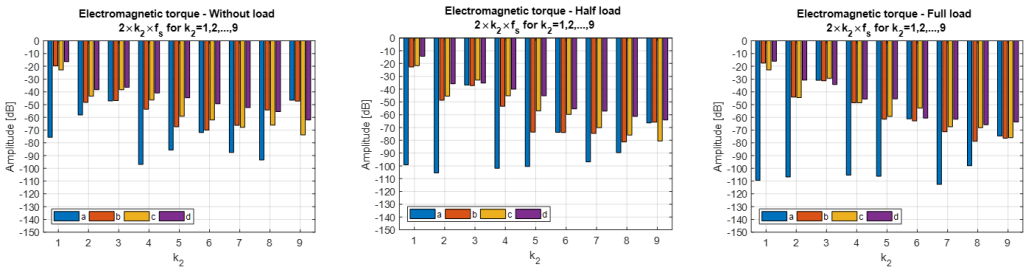

Figure 19: Electromagnetic torque harmonics, (a) healthy machine, (b) 3% unbalanced voltage, (c) 16.6% inter-turn stator winding short-circuit, (d) 33% inter-turn stator winding short-circuit.

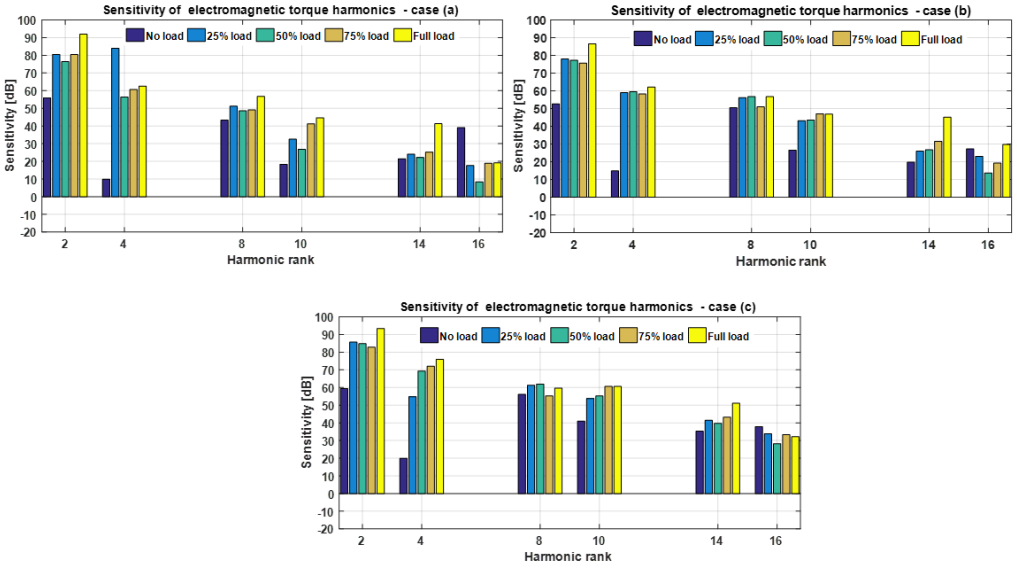

Figure 20: Sensitivity of electromagnetic torque harmonics, (a) healthy machine (b) 3% unbalanced voltage, (c) 16.6% inter-turn stator winding short-circuit, (d) 33% inter-turn stator winding short-circuit.

8. Conclusion

In this paper, a comparative study of three diagnostic methods based on harmonic analysis of stator currents, stay flux and electromagnetic torque has been proposed. The three methods are assessed under the same conditions to detect the same fault to verify their performance. The IM model used in this work is based on the finite element method. This model is a powerful tool to analyses machine behavior and to serve as test-bench with precisely known

and controlled environment.Also, FEM provides a theoretically ideal model where no inherent asymmetries or manufacturing defects are accounted for. From the obtained simulation results, it should be noted that for the stator current method the components of 150Hz, 450Hz and 750Hz in saturation related harmonics at rank $(3k_1 f_s)$ shows a good performances for the detection of inter-turn short-circuit fault. For the electromagnetic torque method the 2^{nd} and 8^{th} harmonics have proved a high sensitivity for detection of this kind of faults. But the drawback of these two methods is their inability to distinguished the inter-turn short-circuit fault from the unbalanced voltage supply. Furthermore, it has been demonstrated that the sensitive harmonics in the stray flux method are the components of 150Hz, 450Hz, 750Hz and 1050Hz in saturation related harmonics and 250Hz, 350Hz, 550Hz and 650Hz in MMF-related harmonics. These signatures have a high ability to detects and distinguish between the inter-turn short-circuit fault and unbalanced voltage supply which lead to a reliable diagnosis system. Finally, this technique is cost effective thanks to the low cost flux sensor needed in the monitoring process.

References

[1] Benbouzid, M.E.H., 1998. A review of induction motors signature analysis as a medium for faults detection, in: IECON '98. Proceedings of the 24th Annual Conference of the IEEE Industrial Electronics Society (Cat. No.98CH36200), pp. 1950–1955 vol.4.

[2] Bentounsi, A., Nicolas, A., 1998. On line diagnosis of defaults on squirrel cage motors using fem. IEEE Transactions on Magnetics 34, 3511–3514.

[3] Cruz, S.M.A., Cardoso, A.J.M., 2001. Stator winding fault diagnosis in three-phase synchronous and asynchronous motors, by the extended park's vector approach. IEEE Transactions on Industry Applications 37, 1227–1233.

[4] Cusido, J., Romeral, L., Ortega, J.A., Rosero, J.A., Garcia Espinosa, A., 2008. Fault detection in induction machines using power spectral density in wavelet decomposition. IEEE Transactions on Industrial Electronics 55, 633–643.

[5] Frosini, L., Borin, A., Girometta, L., Venchi, G., 2011. Development of a leakage flux measurement system for condition monitoring of electrical

drives, in: 8th IEEE Symposium on Diagnostics for Electrical Machines, Power Electronics Drives, pp. 356–363.

[6] Frosini, L., Borin, A., Girometta, L., Venchi, G., 2012. A novel approach to detect short circuits in low voltage induction motor by stray flux measurement, in: 2012 XXth International Conference on Electrical Machines, pp. 1538–1544.

[7] Gentile, G., Meo, S., Ometto, A., 2003. Induction motor current signature analysis to diagnostics, of stator short circuits, in: 4th IEEE International Symposium on Diagnostics for Electric Machines, Power Electronics and Drives, 2003. SDEMPED 2003., pp. 47–51.

[8] Gyftakis, K.N., Spyropoulos, D.V., Kappatou, J.C., Mitronikas, E.D., 2013. A novel approach for broken bar fault diagnosis in induction motors through torque monitoring. IEEE Transactions on Energy Conversion 28, 267–277.

[9] Hsu, J.S., 1995. Monitoring of defects in induction motors through air-gap torque observation. IEEE Transactions on Industry Applications 31, 1016–1021.

[10] Irhoumah, M., Pusca, R., Lefevre, E., Mercier, D., Romary, R., Demian, C., 2018. Information fusion with belief functions for detection of inter-turn short-circuit faults in electrical machines using external flux sensors. IEEE Transactions on Industrial Electronics 65, 2642–2652.

[11] Jardine, A.K., Lin, D., Banjevic, D., 2006. A review on machinery diagnostics and prognostics implementing condition-based maintenance. Mechanical Systems and Signal Processing 20, 1483 – 1510. URL: http://www.sciencedirect.com/science/article/pii/S0888327005001512, doi:https://doi.org/10.1016/j.ymssp.2005.09.012.

[12] Joksimovic, G.M., Penman, J., 2000. The detection of inter-turn short circuits in the stator windings of operating motors. IEEE Transactions on Industrial Electronics 47, 1078–1084.

[13] Karmakar, S., Chattopadhyay, S., Mitra, M., Sengupta, S., 2016. Induction Motor Fault Diagnosis Approach through Current Signature Analysis.

[14] Kokko, V., 2003. Condition Monitoring of Squirrel-cage Motors by Axial Magnetic Flux Measurements. Acta Universitatis Ouluensis: Technica, University of Oulu. URL: https://books.google.fr/books?id=gS4OMwAACAAJ.

[15] Kumar N., P., Isha, T.B., 2019. Fem based electromagnetic signature analysis of winding inter-turn short-circuit fault in inverter fed induction motor. CES Transactions on Electrical Machines and Systems 3, 309–315.

[16] Lamim Filho, P., Pederiva, R., Brito, J., 2014. Detection of stator winding faults in induction machines using flux and vibration analysis. Mechanical Systems and Signal Processing 42, 377–387.

[17] Lamim Filho, P.C.M., Brito, J.N., Silva, V.A.D., Pederiva, R., 2013. Detection of electrical faults in induction motors using vibration analysis. Journal of Quality in Maintenance Engineering .

[18] Liang, X., Ali, M.Z., Zhang, H., 2020. Induction motors fault diagnosis using finite element method: A review. IEEE Transactions on Industry Applications 56, 1205–1217.

[19] Lombard, P., Meunier, G., 1992. A general method for electric and magnetic coupled problem in 2d and magnetodynamic domain. IEEE Transactions on Magnetics 28, 1291–1294.

[20] Lu, B., Habetler, T.G., Harley, R.G., 2008. A nonintrusive and in-service motor-efficiency estimation method using air-gap torque with considerations of condition monitoring. IEEE Transactions on Industry Applications 44, 1666–1674.

[21] Maraaba, L., Hamouz, Z., Abido, M., 2018. An efficient stator inter-turn fault diagnosis tool for induction motors. Energies 11, 653. doi:10.3390/en11030653.

[22] Melero, M.G., Cabanas, M.F., Rojas, C., Orcajo, G.A., Cano, J.M., Solares, J., 2003. Study of an induction motor working under stator winding inter-turn short circuit condition, in: 4th IEEE International Symposium on Diagnostics for Electric Machines, Power Electronics and Drives, 2003. SDEMPED 2003., pp. 52–57.

[23] Negrea, M.D., 2006-11-29. Electromagnetic flux monitoring for detecting faults in electrical machines. URL: http://urn.fi/urn:nbn:fi:tkk-008516.

[24] Penman, J., Sedding, H.G., Lloyd, B.A., Fink, W.T., 1994. Detection and location of interturn short circuits in the stator windings of operating motors. IEEE Transactions on Energy Conversion 9, 652–658.

[25] Pusca, R., Demian, C., Mercier, D., Lefèvre, , Romary, R., 2012. An improvement of a diagnosis procedure for ac machines using two external flux sensors based on a fusion process with belief functions, in: IECON 2012 - 38th Annual Conference on IEEE Industrial Electronics Society, pp. 5096–5101.

[26] Rojas, C., Melero, M.G., Cabanas, M.F., Cano, J.M., Orcajo, G.A., Pedrayes, F., 2007. Finite element model for the study of inter-turn short circuits in induction motors, in: 2007 IEEE International Symposium on Diagnostics for Electric Machines, Power Electronics and Drives, pp. 415–419.

[27] Saad, N., Irfan, M., Ibrahim, R., 2018. Condition Monitoring and Faults Diagnosis of Induction Motors: Electrical Signature Analysis. CRC Press. URL: https://books.google.fr/books?id=f7NjDwAAQBAJ.

[28] Sarma, N., Mohammed, A., Melecio, J.I., Tshiloz, K., Djurović, S., 2016. An experimental study of winding fault induced slot harmonic effects in the cage rotor induction machine stator current, in: 8th IET International Conference on Power Electronics, Machines and Drives (PEMD 2016), pp. 1–6.

[29] Siddique, A., Yadava, G.S., Singh, B., 2005. A review of stator fault monitoring techniques of induction motors. IEEE Transactions on Energy Conversion 20, 106–114.

[30] da Silva, A.M., Povinelli, R.J., Demerdash, N.A., 2013. Rotor bar fault monitoring method based on analysis of air-gap torques of induction motors. IEEE Transactions on Industrial Informatics 9, 2274–2283.

[31] Stavrou, A., Sedding, H.G., Penman, J., 2001. Current monitoring for detecting inter-turn short circuits in induction motors. IEEE Transactions on Energy Conversion 16, 32–37.

[32] Tarchała, G., Wolkiewicz, M., 2019. Performance of the stator winding fault diagnosis in sensorless induction motor drive. Energies 12, 1507.

[33] Thailly, D., Romary, R., Brudny, J.F., 2005. Quantitative analysis of the external radial magnetic field for detection of stator inter-turn short-circuit in induction machines, in: 2005 European Conference on Power Electronics and Applications, pp. 8 pp.–P.8.

[34] Thomson, W.T., 2001. On-line mcsa to diagnose shorted turns in low voltage stator windings of 3-phase induction motors prior to failure, in: IEMDC 2001. IEEE International Electric Machines and Drives Conference (Cat. No.01EX485), pp. 891–898.

[35] Toliyat, H., Nandi, S., Choi, S., Meshgin-Kelk, H., 2012. Electric machines: modeling, condition monitoring, and fault diagnosis. CRC Press.

[36] Toliyat, H.A., Lipo, T.A., 1995. Transient analysis of cage induction machines under stator, rotor bar and end ring faults. IEEE Transactions on Energy Conversion 10, 241–247.

[37] Tumanski, S., 2007. Induction coil sensors—a review. Measurement Science and Technology 18. doi:10.1088/0957-0233/18/3/R01.

[38] Wu, Q., Nandi, S., 2008. Fast single-turn sensitive stator inter-turn fault detection of induction machines based on positive and negative sequence third harmonic components of line currents, in: 2008 IEEE Industry Applications Society Annual Meeting, pp. 1–8.

[39] Ye Zhongming, Wu Bin, 2000. A review on induction motor online fault diagnosis, in: Proceedings IPEMC 2000. Third International Power Electronics and Motion Control Conference (IEEE Cat. No.00EX435), pp. 1353–1358 vol.3.

[40] Zheng Liu, Cao, W., Huang, P., Tian, G., Kirtley, J.L., 2016. Non-invasive winding fault detection for induction machines based on stray flux magnetic sensors, in: 2016 IEEE Power and Energy Society General Meeting (PESGM), pp. 1–6.